Real-Time Inverse Kinematics: The Return of the Jacobian

Michael Meredith & Steve Maddock
Department of Computer Science
University of Sheffield
United Kingdom
E-mail: M.Meredith@dcs.shef.ac.uk, S.Maddock@dcs.shef.ac.uk

KEYWORDS

Inverse Kinematics, Computer Character Animation, Real-time

ABSTRACT

Due to their scalability, numerical techniques often form part of an inverse kinematics solver. However, because of their iterative nature, such methods can be slow. So far research into the field of kinematics has failed to find a general non-numerical solution to the problem. Many researchers have proposed hybrid techniques yet these still rely on a numerical aspect. It is therefore important to find ways of using numerical techniques as efficiently as possible. In this paper we take a look at the Jacobian-based IK solver and techniques that allow this method to be used as an efficient real-time IK solver.

INTRODUCTION

Inverse kinematics is used to determine a set of joint angles in an articulated structure based upon the position of a given node in the hierarchical structure. The problem domain that is tackled by inverse kinematics solvers was first formulated in the mechanical engineering literature [Crai55] and more specifically research into the field of robotics. We are interested in its application in computer character animation. The issue that inverse kinematics attempts to resolve is to find a set of joint configurations of an articulated structure based upon a desirable end-effector location.

There have been many varied techniques used as an inverse kinematics solver. The fastest techniques, such as analytical, tend to suffer from poor scalability whereas the scalable techniques such as numerical iteration, suffer from poor solver times. Many techniques that have been proposed to offer speed advantages utilise numerical solvers therefore it is important to consider ways that such techniques can be used efficiently. A review of many of the present IK techniques is given in the following section.

After a review of techniques, we take a look at what the actual problem IK techniques attempt to solve. This is a primer to the material we subsequently present during which we look at the iterative Jacobian approach to inverse kinematics and discuss techniques that allow the method to used effectively. The following section of the report presents a real-time application that drives a walking character around rough terrain to demonstrate the effectiveness of our Jacobian interpretation. We end the paper by presenting and discussing the results of our work.

RELATED WORK

The problem posed of inverse kinematics has resulted in a variety of different techniques that can be used to yield a desirable result. Of these techniques, 4 different categories of solver can be identified: geometric/analytical algorithms, cyclic co-ordinate descent (CCD), differential techniques and hybrid methods [Tola00] which mix together various aspects of the first three techniques.

The geometric/analytical algorithms [Chin96, Kwan00, Paul88] tend to be very quick because they reduce the IK problem to a mathematical equation that need only be evaluated in a single step to produce a result. The limitations of this class of solver become apparent in the case of large chains. In such cases, the task of reducing the problem to a single-step mathematical equation is impractical. Therefore geometric/analytical techniques tend to be less useful in the field of character animation.

IK solvers that are based on CCD [Eber01, Wang91, Welm93] use an iterative approach that takes multiple steps towards a solution. The steps that the solver takes are formed heuristically, therefore this step can be performed relatively quickly. An example of a possible heuristic would be to minimise the angle between pairs of vectors created when projecting lines through the current node and end-effector and current node and desired location. However, because the iterative step is heuristically driven, accuracy is normally the price paid for speed. Another issue with this technique is that one joint angle is updated at a time as opposed to the complete hierarchical structure of differential-based techniques. This has the undesirable and unrealistic result of earlier joints moving much more than later limbs in the IK chain.

In a similar way to the CCD technique, differential-based techniques [Watt92, Zhao94] utilise an iterative approach that requires multiple steps to find a solution. The steps that the algorithm makes are determined via the use of the system Jacobian that relates small changes in joint configurations to positional offsets. Since all the joint angles are updated in a single

step, the movements are dissipated over the whole chain which results in a more realistic looking posture.

By their nature, iterative-based techniques are generally slower at producing desirable result when compared to their analytical counterparts. However the problem with the analytical methods is their lack of scalability. Fedor [Fedo03] explores this trade-off between speed, accuracy and scalability in an IK solver. One of the results from this work demonstrates that differential-based numerical solutions, although slower than both CCD and analytical techniques, provide better results for larger chains. This highlights the importance of refining numerical techniques such that we maintain accuracy and scalability but drive solution time down.

One such solution proposed by Tang *et al* [Tang99] makes use of the SHAKE algorithm [Ryck77] to achieve a fast iterative-based IK solver. This technique treats a hierarchical structure as point masses that are related by system constraints. This is in contrast to the Jacobian-based technique that encapsulates the articulated information and thereby provides us the cohesion between links for free.

In order to achieve a desired end-effector location, the mass points of the SHAKE system are adjusted per cycled until a global goal has been reached. This includes meeting a threshold of acceptable error on the constraints. However because of the lack of node dependency of the algorithm, normally the points will lose their distance relationships between each other. To counter this issue, correcting forces are iteratively applied to each point to reassert cohesion between links therefore the accuracy of parent-child distances directly effects solver time. Without a reasonable level of accuracy at this point, the appearance of rigid links moving about each other would occur. This is an issue that the Jacobian-based techniques are not affected by.

The time complexity of the SHAKE algorithm is suggested by Tang *et al* to be $O(n^2)$ with respect to the number of constraints. However since each link in a hierarchical chain requires a constraint to impose cohesion, the time to solve a system is also minimally $O(n^2)$ with respect to the number of links in the chain. The inclusion of additional system constraints such as joint angle limits has a further detrimental effect on solution time therefore making the algorithm less applicable to real-time applications as the number of links increase.

Another real-time IK technique proposed by Shin *et al* [Shin01] that is used for computer puppetry makes use of a hybrid solution. This technique attempts to use analytical solutions where possible, except in cases where a large amount of body posturing is required, where a numerical implementation is invoked. The numerical solver only acts upon the IK chain defined between the root and the upper body while the analytical solver is used for the limbs of the character.

The hybrid use of IK solvers used by Shin *et al* demonstrates a good method for performing real-time IK however the analytical aspect assumes some knowledge about the character's structure [Lee99, Tola96]. This means that the overall IK technique is not a general one that can be applied to arbitrary IK chains. The other potential problem with the hybrid technique is similar to the CCD techniques in that not all joint angles are updated simultaneously which means unrealistic and unproportional posture configurations could result.

From the research done in the field of real-time IK, it is apparent that analytical solutions by themselves are just not scalable enough to meet much of the demands of modern computer-based IK problems. Therefore numerical techniques are used as either a substitute or in serial with an analytical solution which serves to highlight the importance of having fast numerical solutions. Furthermore these solutions should operate on the whole hierarchical structure equally to avoid unrealistic postures. These are the issues we address with our Jacobian-based approach for real-time IK.

PRIMARIES

Kinematics

The application of kinematic algorithms for character animation is used to posture articulated creatures based on a simple definition of joint angles and limb lengths. These creatures may take practically any form from humanoid bipedal characters to quadruped animals to just about anything that can be imagined using a hierarchal structure.

Structures described using a hierarchical form are defined using a parent-child system similar to that of tree structures. In the case of computer characters, each rigid limb of the structure is a child node in the tree whose parent node provides a reference point from which it is described. The parents are themselves child nodes of limbs above in the hierarchy and this recursive relationship continues up to a root node. The parent of the root node is effectively taken as the global frame of reference and defined as such.

At the other end of the tree are leaf nodes which are children that have no descendants of their own. An End-effector in terms of kinematic chains is any node within the hierarchy that an animator wishes to directly position, for example to interact with the environment. End-effectors are commonly the leaf nodes of an articulated structure as it is the feet and hands that generally interact with the world.

The definition of each node within the structure is simply an offset from its parent's local centre of reference, a rotation about a locally defined axis and an object to display. In the case of rigid body animation, the limbs are non-prismatic so the offset parameters are considered as constants. Therefore in order to define a character's posture the orientation parameters are the only changeable settings plus the global position of the root node. Figure 1.1 illustrates a humanoid hierarchal structure where the root node is the *Hips* whose children are the *Chest, LeftHip* and *RightHip* limbs. End-effectors of the articulated character in Figure 1.1 consist of the *Head, Hands* and *Feet*.

There are two distinct variations of kinematic control called forward and backward (or inverse) which are used to achieve very different goals. However in many areas of character animation they coexist to aid in the production of a complete structural definition. These are described in detail in the following subsections.

Forward Kinematics

From the definition of nodes within a hierarchy there are very few parameters to set for each node, namely an orientation and offset from its parent. Specifying all of these parameters for each node within the hierarchy is termed forward kinematics.

When calculating the complete posture of a character, the defined parameters of parent nodes effect the absolute locations of its children thereby creating a propagation effect of parent settings. The rippling effect of parameters starts with the root and spreads outwards through the hierarchy to its children, grandchildren, and so on. Therefore by the time a leaf node is reached, its absolute location is calculated based on its local orientation and offset plus all of its ancestors' local orientations and offsets. This leads to Equation 1.1 for defining forward kinematic structures where θ represents the complete set of orientation values for a structure and X is the global position of a given limb in the hierarchy.

$$X = f(\theta) \qquad\qquad (1.1)$$

An advantage of hierarchically defined structures lies in the ability to locally orientate a character's limbs by setting its local orientations thereby eliminating problems of aligning and maintaining segment relationships. The principle of forward kinematics allows a character's posture to be easily set up using a parameter copy of a similarly structured character which will result in a good natural looking pose albeit perhaps not entirely accurate to the environment.

A limitation of the forward kinematic technique is the inability to easily position limbs at absolute positions in space, for example to touch an object in space. This drawback arises because a limb is only orientated locally with respect to its parent therefore the absolute position depends on all of its parents. For short child-parent relationships from the desired limb to the root (termed a chain) this issue is not too much of a problem because it is possible to image the path and with a little foresight set the orientation values of the limbs. However for larger chains, this requires much trial and error to get a realistic posture. This is where inverse kinematics (IK) techniques prove to be an invaluable tool in character animation.

Inverse Kinematics

The principle behind inverse kinematics reverses that of forward kinematics and as opposed to determining absolute limb positions given joint orientations, joint orientations are calculated based on absolute limb positions. Usually only the leaf nodes need to be positioned in space. However, any limb within the hierarchy can be position using this technique.

The usefulness of this tool becomes apparent when characters interact with the environment, like grasping a mug, because instead of imaging what the chain will look like in order to configure the character as in the case of forward kinematics, all inverse kinematics
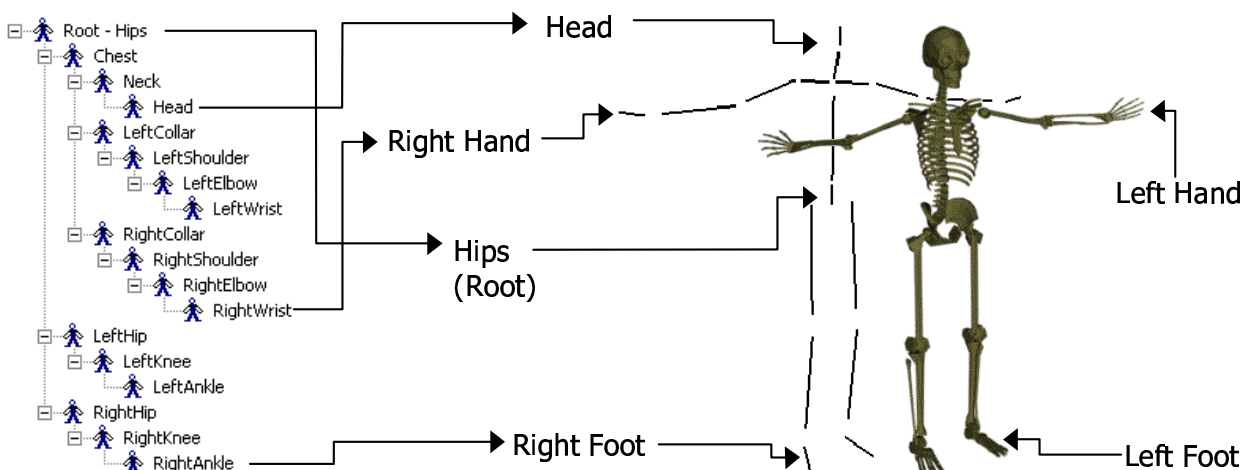

Figure 1.1: Hierarchically Defined Humanoid Character

requires is the location of the mug in space. The mathematical representation of the inverse kinematics technique is defined in Equation 1.2.

$$\theta = f^{-1}(X) \qquad (1.2)$$

Through the combined use of forward and backward kinematics, animators have the freedom and flexibility to pose characters easily. However, inverse kinematics is not as simple a process as forward kinematics and much work has gone into finding a quick and accurate solution to the problem. The next section presents our approach.

OUR INVERSE KINEMATICS SOLUTION

Jacobian Inverse Kinematics

Our implementation of inverse kinematics is based upon the well-established Jacobian technique. The objective of this technique is to incrementally change joint orientations from a stable starting position towards a configuration state that will result in the required end-effector being located at the desired position in absolute space. The amount of incremental change on each iteration is defined by the relationship between the partial derivatives of the joint angles, θ, and the difference between the current location of the end effector, X, and the desired position, X_d. The link between these two sets of parameters leads to the system Jacobian, J. This is a matrix that has dimensionality $(m \times n)$ where m is the spatial dimensional of X and n is the size of the joint orientation set, θ. The Jacobian is derived from Equation 1.1 as follows. Taking partial derivatives of Equation 1.1:

$$dX = J(\theta)d\theta \qquad (1.3)$$

where

$$J_{ij} = \frac{\partial f_j}{\partial x_i} \qquad (1.4)$$

Rewriting Equation 1.3 in a form similar to inverse kinematics (Equation 1.2) results in Equation 1.5. This form of the problem transforms the under-defined system into a linear one that can be solved using iterative steps.

$$d\theta = J^{-1}dX \qquad (1.5)$$

The problem now is that Equation 1.5 requires the inversion of the Jacobian matrix. However because of the under-defined problem that the inverse kinematics technique suffers from, the Jacobian is very rarely square. Therefore, in our implementation we have used the right-hand generalised pseudo-inverse to overcome the non-square matrix problem, as given in equation 1.6.

Generating the pseudo-inverse of the Jacobian in this way can lead to inaccuracies in the resulting inverse that need to be reduced. Any inaccuracies of the inverse Jacobian can be detected by multiplying it with the original Jacobian then subtracting the result from the identity matrix. A magnitude error can be determined by taking the second norm of the resulting matrix multiplied by dX, as outlined in Equation 1.7. If the error proves too big then dX can be decreased until the error falls within an acceptable limit.

An overview of the algorithm we used to implement an iterative inverse kinematics solution is as follows:

1) *Calculate the difference between the goal position and the actual position of the end-effector:*
$$dX = X_g - X$$
2) *Calculate the Jacobian matrix using the current joint angles: (using Equation 1.4)*
3) *Calculate the pseudo-inverse of the Jacobian:*
$$J^{-1} = J^T(JJ^T)^{-1} \qquad (1.6)$$
4) *Determine the error of the pseudo-inverse*
$$error = \left\| (I - JJ^{-1})dX \right\| \qquad (1.7)$$
5) *If error > e then*
$$dX = dX / 2$$
restart at step 4
6) *Calculate the updated values for the joint orientations and use these as the new current values:*
$$\theta = \theta + J^{-1}dX$$
7) *Using forward kinematics determine whether the new joint orientations position the end-effector close enough to the desired absolute location. If the solution is adequate then terminate the algorithm otherwise go back to step 1.*

The computational demand of the algorithm is relatively high over a number of iterations, so well-defined character hierarchies are advantageous. This means that each node in the articulation is defined by the minimum number of degrees of freedom (DOF) required thereby making θ as small as possible. For example, pivot joints such as an elbow would only be modelled using a single DOF whereas a ball and socket joint like the shoulder would need 3 Euler DOFs to represent the range of possible movements.

The use of well-defined hierarchies further helps to prevent the inverse kinematics solver from producing unnatural-looking postures. However this still does not cover all of the potential unnatural poses the solver can return. In order to restrict the IK solver to the orientation space of only possible character configurations, joint orientation restrictions can be enforced within the scope of the existing algorithm. The simplest way of incorporating such constraints is to crop the joint angles.

This requires Step 6 of the algorithm to be modified in the following way:

6) *Calculate the updated values for the joint orientations and use these as the new current values:*

$$\theta = \begin{cases} lowerbound & if \quad \theta + J^{-1}dX < lowerbound \\ upperbound & if \quad \theta + J^{-1}dX > upperbound \\ \theta + J^{-1}dX & otherwise \end{cases}$$

The time to complete the IK algorithm for a given end-effector is an unknown quantity due to an arbitrary number of iterations required. However the time to complete a single iteration is constant with respect to the dimensionality of X and θ which is unchanged under a complete execution of the algorithm. Therefore by placing an upper limit on the number of iterations we can set a maximum time boundary for the algorithm to return in. If the solver reaches the limit then the algorithm returns the closest result it has seen.

In 3-dimensional space, the dimensionality of X in a Jacobian-based inverse kinematics solver is generally either 3 or 6. The 6-dimensional X vector is normally used as it contains both positional and orientation information whereas a 3-dimensional vector only contains positional information for an end-effector.

From the inverse kinematics algorithm outlined above, it is clear that the 3-dimensional X vector is quicker over its counterpart and should always be used when orientation is not required. However there are times that orientation is required but it is still possible to use the 3-dimensional vector which is demonstrated in our application of the algorithm present later.

To see how much of a cost difference there is between the two sizes of X vector, the corresponding complexity analysis of them is illustrated in the following section.

Complexity Analysis Of The *X* Vector

So far we have not specified what technique is used to perform the inverse of the square matrix JJ^T that forms part of the pseudo-inverse of the Jacobian (Equation 1.6). Depending on whether the X vector is either a 6- or 3-dimensional vector, the JJ^T matrix will have dimensionality (6 x 6) or (3 x 3) respectively. For the 3-dimensioned matrix an analytical solution is readily derivable however the larger matrix is better suited with a numerical solution. For our purposes we have used an LU decomposition algorithm for the (6 x 6) matrix and analytical inversion for the (3 x 3) matrix. The complexities of both techniques are now outlined.

LU Decomposition and Analytical Inversion
LU decomposition can be used to determine the inverse of a square matrix by using the matrix identity, $AA^{-1} = I$,

where I is an identity matrix (and in this case it has dimensionality (6 x 6)). The application of LU decomposition to this equation requires matrix A to be split into 2 further matrices that have the form of lower and upper matrices as illustrated in Equation 1.8.

$$A = LU = \begin{bmatrix} 1 & 0 & 0 & \cdots & 0 \\ * & 1 & 0 & \cdots & 0 \\ * & * & 1 & \cdots & 0 \\ \vdots & \vdots & \vdots & \ddots & \vdots \\ * & * & * & \cdots & 1 \end{bmatrix} \begin{bmatrix} * & * & * & \cdots & * \\ 0 & * & * & \cdots & * \\ 0 & 0 & * & \cdots & * \\ \vdots & \vdots & \vdots & \ddots & \vdots \\ 0 & 0 & 0 & \cdots & * \end{bmatrix}$$

$$(1.8)$$

Our algorithm for decomposing the original (6 x 6) matrix A into its upper and lower components is given in Appendix A. From this code, the complexity of the decomposition can be calculated as being 151 floating-point operations (flops): 55 multiplications, 16 divisions and 80 additions & subtractions.

The decomposition of A into the two matrices allows the original matrix identity to be rewritten into the form of Equation 1.9, which can be easily solved.

$$LUA^{-1} = I \quad \Rightarrow L(UA^{-1}) = I$$
$$\Rightarrow LY = I \quad \textbf{(1.9a)}$$
$$\wedge UA^{-1} = Y \quad \textbf{(1.9b)}$$

The first step is to solve Y from Equation 1.9a which rewrites into a set of n linear equations where n is the number of cols/rows in the inverse matrix; in this case, $n=6$. Due to the nature of the lower matrix, the n linear equations are already in the form that allows a simple forward substitution technique to be applied. Once Equation 1.9a has been solved, Equation 1.9b can be solved to find A^{-1} using a similar technique that also results in a set of n linear equations. Again, because of the form of the upper matrix, the resulting simultaneous equations can be solved using a backward substitution algorithm. Appendix B gives the code we used to solve the equations in Equation 1.9.

The complexity for this part of the inverse algorithm for a (6 x 6) matrix is calculated at 468 flops: 180 multiplications, 36 divisions and 252 additions & subtractions.

Adding together the analysis of the two parts of the LU decomposition results in the total complexity of 619 flops for a (6 x 6) matrix inversion.

In comparison, the analytical inversion of a (3 x 3) matrix is given in Equation 1.10. This inversion can be encoded using the fragment of C++ source code given in Appendix C. The complexity of this is 51 flops: 36

multiplications, 1 division and 14 additions & subtractions.

$$
\begin{bmatrix} r_{00} & r_{01} & r_{02} \\ r_{10} & r_{11} & r_{12} \\ r_{20} & r_{21} & r_{22} \end{bmatrix}^{-1} =
$$

$$
\frac{\begin{bmatrix} r_{11}r_{22} - r_{21}r_{12} & r_{21}r_{02} - r_{01}r_{22} & r_{01}r_{12} - r_{11}r_{02} \\ r_{20}r_{12} - r_{10}r_{22} & r_{00}r_{22} - r_{20}r_{02} & r_{10}r_{02} - r_{00}r_{12} \\ r_{10}r_{21} - r_{20}r_{11} & r_{20}r_{01} - r_{00}r_{21} & r_{00}r_{11} - r_{10}r_{01} \end{bmatrix}}{r_{00}(r_{11}r_{22} - r_{12}r_{21}) + r_{01}(r_{12}r_{20} - r_{10}r_{22}) + r_{02}(r_{10}r_{21} - r_{11}r_{20})}
$$

$$\textbf{(1.10)}$$

The decision to use an analytical solver for the smaller matrix and LU decomposition for the larger one is demonstrated in the Figure 1.2. The results given in Figure 1.2 were obtained using a matrix with all elements non-zero so the analytical technique was unable to make use of zeros to cut off the co-factor expansions. This is a valid assumption because it would be most unlikely that the (6 x 6) matrix that needs to be inverted in the pseudo-inverse would actually contain any zeros.

Figure 1.2 shows the analytical approach to solving matrix inversion is only better for matrices that have dimensionality equal to or less than 3. After this size, the number of flops required to solve an analytical inverse increases in a cubic fashion with respect to dimensionality whereas the LU technique increases at the lower squared rate. This analysis justifies the use of an analytical solution for the (3 x 3) matrix while using LU decomposition for the inversion of the larger (6 x 6) matrix.

Calculating The Jacobian

If the Jacobian definition of Equation 1.4 is divided by a differential time element, the resulting equivalence provides a mapping between angular velocities in state space, θ, and linear velocities in Cartesian space, X. This result is illustrated in equation 1.11.

$$\dot{X} = J(\theta)\dot{\theta} \qquad \textbf{(1.11)}$$

In the case of a 6-dimensional X vector, $\dot{X}$ consists of linear velocity, V, and angular velocity, Ω, components, whereas the 3-dimensional X vector only includes the linear velocity. Both the linear velocity and angular velocity are with respect to a global frame of reference as too are the partial derivatives of the Jacobian. The Jacobian linking the linear and angular velocity of the end-effector, with the intermediary local angular velocities, is given in equation 1.12, where there are i DOFs in the IK chain.

$$
\begin{bmatrix} V \\ \Omega \end{bmatrix} = \begin{bmatrix} b_1, b_2, ..., b_i \\ a_1, a_2, ..., a_i \end{bmatrix} \begin{bmatrix} \dot{\theta}_1 \\ \dot{\theta}_2 \\ \vdots \\ \dot{\theta}_i \end{bmatrix} \qquad \textbf{(1.12)}
$$

In Equation 1.12, the a components are of the local axes for a given link transformed into the global frame of reference. The b elements of the Jacobian are the cross products of the corresponding a axis with the spatial difference between the global origin of the current limb and the absolute location of the end of the articulation, P_e (Equation 1.14). The DOFs within the state space are normally ordered such that limbs from the root are
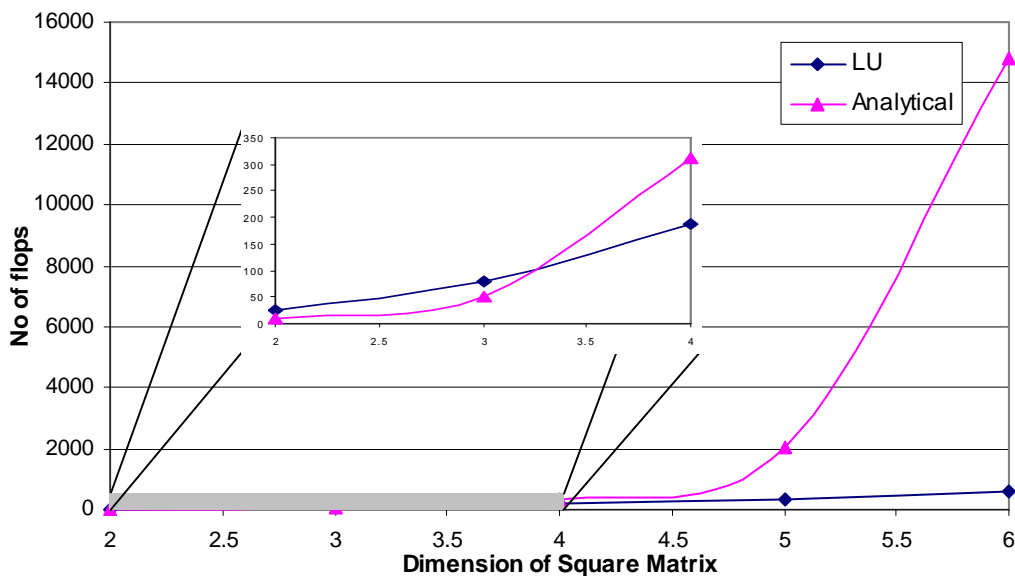
Figure 1.2: Demonstration of the complexity of solving a square matrix using an analytical and LU decomposition technique.

considered first followed by their children, following this pattern to the end of the chain. Using this pattern, the orientation values of the required axes for each limb can be obtained from a transformation matrix, ^0T_j, that converts points defined in the limb's local orientation into a global position. Equation 1.13 illustrates this for the jth limb in the IK chain (note that this assumes a right-handed coordinate system):

$$^0T_j = \begin{bmatrix} a_{xj} & a_{yj} & a_{zj} & P_j \\ 0 & 0 & 0 & 1 \end{bmatrix} \quad \textbf{(1.13)}$$

The parameter P_j in Equation 1.13 also gives the global position of the origin of the limb thereby aiding in the determination of the b components in Equation 1.14.

$$b = a_i \times (P_e - P_j) \quad \textbf{(1.14)}$$

Using the chaining principle for calculating the transforms of the local axes into a global reference frame ($^0T_{j =} {}^0T_1 \text{ x } {}^1T_2 \text{ x } \ldots \text{ x } {}^{j-1}T_j$.), the direct implementation of this subsection in 3-dimensional space yields a constant complexity. Assuming that each link has 3 DOFs, the complexity associated with each limb in the IK chain is given by 162 flops: 98 multiplications and 64 additions & subtractions. The assumption of 3 DOFs does not add a great deal of complexity if it is an overestimate since each DOF contributes only 9 flops to the overall result (where the 9 flops is the calculation of the cross product).

Determining The Pseudo-Inverse Of The Jacobian

Using the complexity derivation of the inversion of a square matrix from the above sections, the complexity of the pseudo-inverse of the Jacobian, as given in Equation 1.6, can be easy calculated. Table 1.1 outlines the number of flops required to calculate the pseudo-inverse depending on the size of the X vector. The variable n is the size of the state space, θ (i.e. the sum of all the links' DOFs). It should also be noted that there is no inclusion of complexity to calculate the transpose of matrices when they are required as this can be handled at no extra cost be simply swapping out indexing parameters.

Size of *Matrix* Operation	(3 x n) 3D *X* Vector	(6 x n) 6D *X* Vector
$A = JJ^T$	18n – 9	72n – 36
$B = A^{-1}$	51	619
$J^T B$	15n	33n
$J^{-1} = J^T (JJ^T)^{-1}$	33n + 42	105n + 583

Table 1.1: Number of flops required to calculate the pseudo-inverse of a non-square matrix.

Complexity Of The Whole IK Solver

The complexity of a single loop of the IK algorithm described above can be derived using the complexity analyses of the smaller parts of the algorithm already determined. This is shown in Table 1.2 where m is the number of inner loops executed at stage 5 of our algorithm.

As Table 1.2 illustrates the use of a 3-dimensional X vector appears to be about 2½ times less computationally demanding than its 6-dimensional counterpart. Considering only the major factor of the complexity, which is the size of the state space, n, the 3-dimensional X vector should be 238.9% quicker than the alternative. However, the complexity of each algorithm is not only dependent on the size of the state space but also on the number of inner loops which are required to make the inversion of the Jacobian stable enough to provide meaningful results. Therefore it needs to be shown that the use of a smaller Jacobian in the 3-dimensional X vector case does not adversely affect the pseudo-inverse. This does not appear to be the case as illustrated with the empirical dataset present in the following section.

So, since the smaller X vector can be shown to be less computationally demanding by a significant factor, it raises the question of whether the smaller X vector can be used even when orientation is important? The following section proves this is possible

Size of X Vector Algorithm Stage	3		6	
1. Calc. increment		3 flops		6 flops
2. Calc. Jacobian		162 flops		162 flops
3. Calc. Pseudo-Inverse	33n +	42 flops	105n +	583 flops
4. Check for convergence	18n +	15 flops	72n +	66 flops
5. Reduce *dX*	18m	flops	72m	flops
6. Update joint angles	6n	flops	12n	flops
7. Calc. new position	38n	flops	38n	flops
Total	95n + 18m + 252 flops		227n + 72m + 817 flops	

Table 1.2: Complexity analysis of our Jacobian based IK solver

USING THE HALF- OVER THE FULL-JACOBIAN

An obvious application of the half-Jacobian is in applications that do not discriminate against the orientation of the final link in an inverse kinematics chain. In applications of inverse kinematics where the orientation of the end-effector has little consequence, the 3-dimensional *X* vector should always be used to reduce the computation effort required. For example, when configuring a spider's legs using IK, because the spider effectively walks on the tips of its legs, the orientation of this end point is immaterial therefore only the 3-dimensional *X* vector would be required. As illustrated in Table 1.2, using the full-sized Jacobian in such cases would be less efficient than the half-sized Jacobian.

Another, more subtle, application of the half-sized *X* vector is in situations where the penultimate link in the IK chain has unlimited and full use of all 3 DOFs (in 3 dimensional space). In this scenario the first step is to calculate the position of the penultimate link based on the desired position and orientation of the final node. The 3-dimensional *X* vector can then be used to position the penultimate node in the chain. Once this is done the desired orientation of the final node can be specified thereby allowing the correct end configuration of the chain.

Other applications where the half-size Jacobian would prove a better technique to employ over the full-size version is in situations of low resolution modelling. For example, if a complex articulated model is being animated as a background entity in a scene, it would be advantageous to switch to the quicker half-Jacobian to solve its configuration. This means that more avatars can be animated in the background of a scene.

There are many other applications where the half-sized Jacobian could substitute for the traditional full-sized version. Currently we have applied the quick half-Jacobian inverse kinematic solver to motion capture retargetting and IK-driven character walking. Both of these applications can easily run in real-time as demonstrated in the following section which describes the latter of our applications.

IK-GENERATED HUMANIOD WALKING

The coupling of a procedural model and an inverse kinematics solver provides the basic building blocks needed to generate the walking motion of a computer character. The procedural model describes the path through which the foot travels during a stride while the IK solver positions (and orientates) the foot along this path over time. The task of tracing the foot along the path would initially appear to require the full-sized Jacobian, inherently requiring the foot to be orientated in a forward facing direction. Without the orientation of

the foot taken into account, there are an infinite number of anatomically correct positions the heel could take in order to meet a simple positional constraint. This is possible because the hip joint for a leg can rotate about the axis of the femur approximately ±90 degrees from the forward facing pose, as illustrated in Figure 1.3.
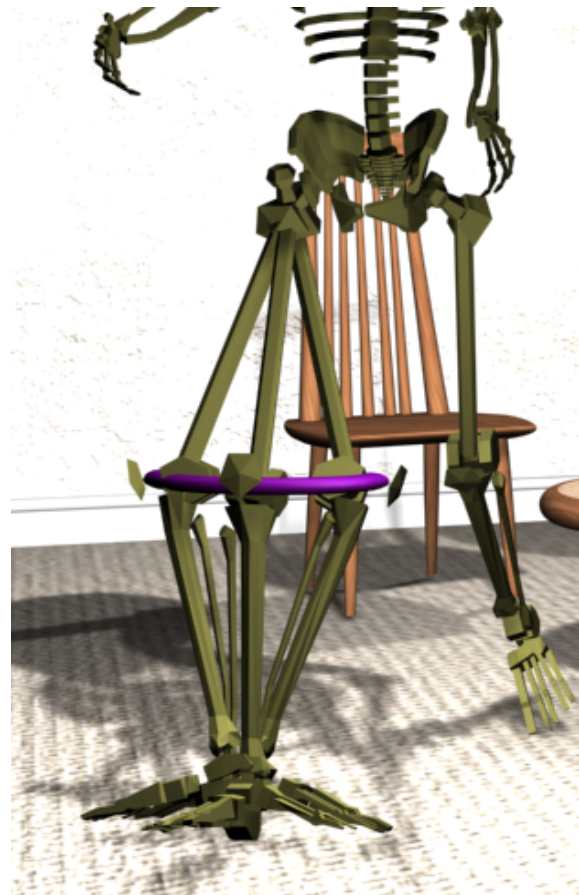
Figure 1.3: Infinite number of positional solutions to fixing a heel plant without regard to the orientation of the foot. The purple ring shows the location of all possible knee positions.

From the evidence of Figure 1.3, it would seem that the full-sized Jacobian is the only choice of IK solver to drive the walking motion of a humanoid character. However, by realising that in the course of a walking motion, any large hip joint rotations result in unnatural postures, additional constraints can be added to restrict movement to only plausible ranges. This would allow the smaller Jacobian to be used to calculate the position of the heal and thus simultaneously reduce the potential for orientation error and increase the performance of the solver.

This approach has been used in our implementation of an IK-driven humanoid character. The following sections present results and comparisons with the conventional full-Jacobian for both performance and realism.

Generating Motion

Our IK-driven character walker, called *MovingIK*, is separated into two main layers. At the bottom level there is the *Animation Layer* that includes the inverse kinematics engine and the procedural stride. Sitting above this level is the *Control Layer* that sets up the parameters required by the *Animation Layer*. Both layers are outlined below. The coupling between the two layers to produce a walking motion is described after the Control layer.

The Animation Layer
The inverse kinematics component of the Animation layer was implemented as a switchable module so that either the half- or the full-sized Jacobian could be easily used. The implementation of the IK solver is a direct encoding of the algorithm described above in the Jacobian Inverse Kinematics section.

The source for the procedural stride model in our application comes from a simple mathematical equation that is illustrated in Equation 1.15. The graphical representation of the procedural stride is illustrated in Figure 1.4 where a complete cycle ranges between 0 and 3π.

If $x \leq \pi$
$$Y = 1 - \cos(x)$$
else
$$Y = 1 - \cos\left(\frac{\pi + x}{2}\right) \qquad \textbf{(1.15)}$$
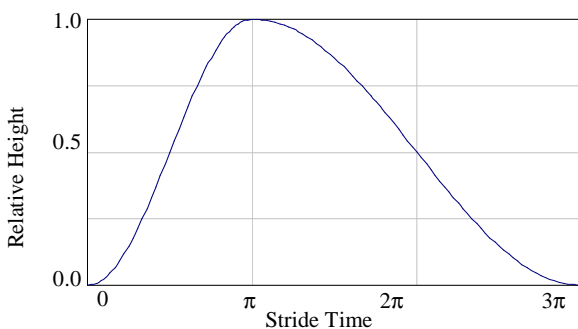
Figure 1.4: Graph of procedural stride based on Equation 1.15

Over uneven terrain this curve is rotated to make the end points of it match up with the height of the heel at the start and the height of the ground at the end of the walk cycle.

Along with the procedural model used to drive the character's foot through the air, we have a pre-flight stage that rolls the foot from a heel supporting phase to a complete foot supporting phase. This uses the inverse kinematics algorithm to simultaneously plant the heel of

the character and gravitate the toes towards the ground. This extra bit of the walking cycle increases the realistic-looking nature of the resulting animation and gives us the ability to model the complete foot as opposed to just the heel. On overview of this procedure is outlined in Figure 1.5 and Table 1.3.

The Control Layer
The responsibility of the control source is to read input from an analogue source that is control by the user and provide the Animation layer with all of the initial values it requires to generate a motion. Such parameters include stride length, stride speed, direction of travel and details about the terrain immediately surrounding the character in order to rotate the stride curve.

Using the values that the Control Level passes down, the Animation layer generates the walking stride. This first includes the pre-flight motion followed by the actual heel flight using the procedural model.

Making the Character Walk
There are two cases under which the character can move forward; walking in a straight line or turning. The Control layer uses input from either an analogue joystick or keyboard to determine the way the character moves. If there is no sideways movements then the walking forward technique is used otherwise a turning action is executed.

- *Move the character forwards*
When the Control later receives a joystick movement it calculates the stride length and speed based on the analogue input. The maximum stride length is half the leg length plus the distance the trailing leg is from the hips in a horizontal direction. The hips of the character only move half this distance because each leg only moves once for every 2 complete walking cycles (i.e. left leg cycle followed by a right leg cycle).

The stride time represents the temporal window used to complete stage (a) of the walking cycle of Figure 1.5. The time to complete stage (b) of Figure 1.5 is dependent on the distance the front toes are from the ground at the end of the first stage. Using the distance between the ground and the toes, the hips of the character are moved by an equal magnitude along the direction of travel. The time to perform the final stage is calculated using this distance value and the velocity of the character from stage (a). Such a timing system is used to decouple the animation speed from the physical frame rate.

While walking forward, the leg that will be trailing behind is fixed to the floor by the toes of the foot while the heel of the foot leading is lifted off the ground and follows the procedural path given in Equation 1.15 in the vertical direction. The other dimensional components
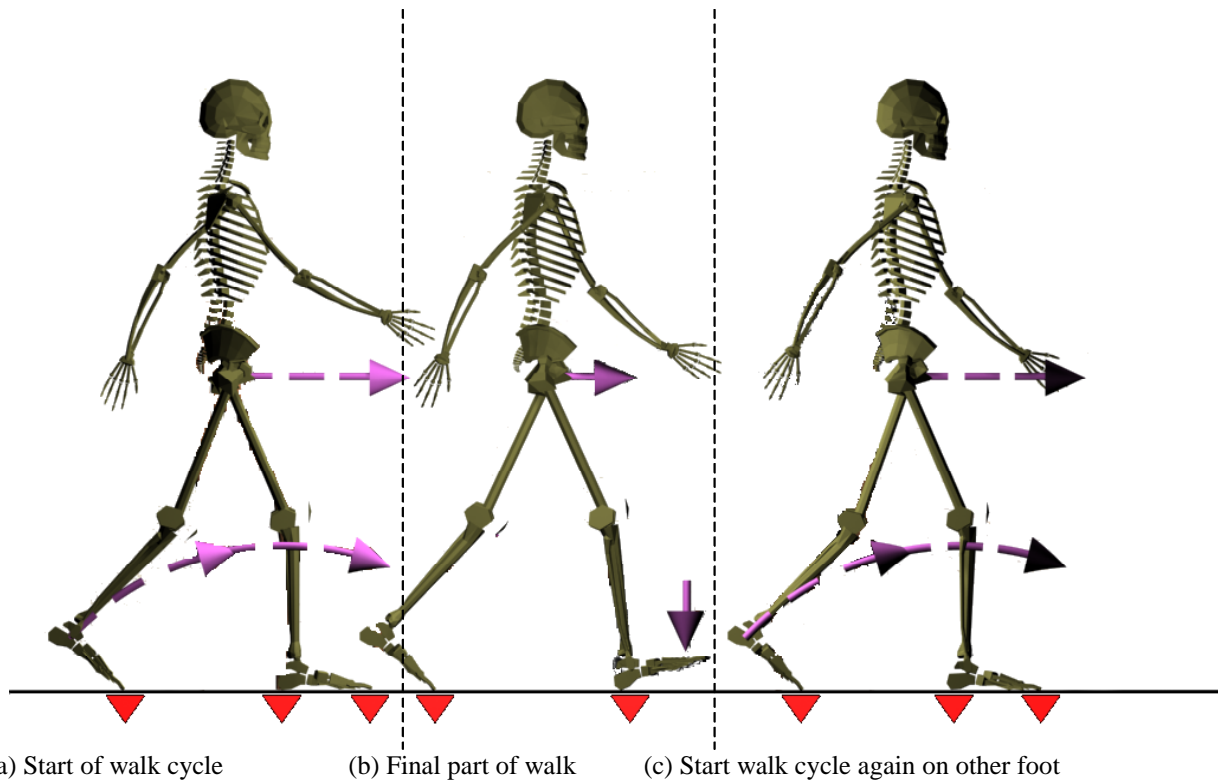
(a) Start of walk cycle   (b) Final part of walk   (c) Start walk cycle again on other foot

Figure 1.5: Demonstration of the cycles implementing in our system. Each frame represents the start of the cycle with the arrows pointing in the direction of travel the node will take until it reaches the start of the next part of the cycle. The red triangles represent plants of the character's limbs.

Stage Description	(a)	(b)
Starting Configuration		
• Left Foot	Both heels and toes are planted on the floor	Toes are planted on the floor
• Right Foot	Toes are planted on the floor	Heel is planted on the floor
Movement	1. Hips move forward, 2. Right heel is advanced forward through the air, 3. Only the left toes remain planted.	1. Hips move forward, 2. Right toes are gravitated towards the floor, 3. Left toes remain planted to the floor

Table 1.3: Illustration of the 2 stage walk cycle where the initial configuration is with the left foot in front and the right foot behind the body.

are driven in a direction parallel to the direction of the walking direction. A linear percentage of time is used to determine how far along the path the foot should be and the Inverse Kinematics solver is used to position the heel to that point, while in a separate application of the solver the toes are clamped to the floor for the trailing foot.

Once the toes of the back foot are clamped to the ground there is enough freedom within the constraints of the human body for the back heel to be lower than the toes and hence penetrate the floor. In order to eliminated this impossible pose, the position of the back heel is checked against the height of the floor at that point. If the heel is lower than the floor a separate algorithm is used to calculate the position that the heel would have to be in

such that the position of the toes are maintained but allowing the heel to be repositioned onto the surface of the floor. Similarly, when the front heel is positioned along the curve, there is the possibility that the toes of the foot will penetrate the floor so this is checked and adjusted to reposition them just on the surface while maintaining the heel position.

When the appropriate amount of time has transpired for the first stage of the step cycle, the heel of the front foot will be in contact with the floor as will the trailing toes and it is time to initiate the second stage. The purpose of stage (b) is to maintain both the current heel and toe plants and gravitate the toes on the front foot towards the ground while still moving the character in a forward

direction. At this stage, the front heels and back toes remained clamped to the floor while the hips continue to move. The front ankle orientation is also adjusted linearly such that at the end of the new temporal window the toes will be in contact with the floor too and thus preparing the character to start a step cycle on the other foot.

- *Making the character turn*

The foot planting phase of making the character walk in an arc is similar to that used to make it walk in a straight line. The vertical component of the leg lifting process is identical to that of walking in a straight line. However instead of making the character walk in a straight line in the direction the character is facing, both the hips and the leading leg's motion is described as a curve in the horizontal plane. The curves that the limbs follow are describe by a centre of rotation, radius and angular difference. With the turning radius determined based on the sharpness of turn, the centre of the circle can be calculated as well as an angular difference which will be linearly interpolated to give the corresponding position in time. We will now outline how the turning centre of the arc is calculated.

The equation for a circle whose origin is located at (Cx, Cy) is given in Equation 1.16 where $0 \leq \theta \leq 2\pi$:

$$(X,Y) = (Cx - r\cos\theta, Cy + r\sin\theta)$$
$$(1.16)$$

The character's location must lie on this circle so (X, Y) can be taken to be the current location of the hips projected onto the horizontal plane. This allows Equation 1.16 to be rearranged to give Equation 1.17 thereby making the centre of the circle the subject:

$$(Cx, Cy) = (X + r\cos\theta, Y - r\sin\theta)$$
$$(1.17)$$

This still leaves θ as an unknown variable in the system of equations, but θ can be calculated by realising that it is the amount the character has already turned from a fixed axis. In our work, we take this axis to be the global Z-axis and therefore θ can be calculated by taking the arc sin of the X component of the normalised forward-facing direction vector of the character. When the character is turning in an anticlockwise direction about the Y-axis, this angle can be directly plugged into the above equation. However when the character is to turn in a clockwise direction about the Y-axis, the angle needs to be negated. This process is illustrated in Figure 1.6.

Once the centre of rotation has been determined, the next stage is to calculate how many degrees the character should be rotated. This is achieved though the use of Equation 1.18 that links properties of an arc where s is

the arc length, θ is the number of radians subscribing the arc, and r is the radius of the arc.

$$s = r\theta \qquad (1.18)$$

With the radius fixed and setting the arc length to be the magnitude displacement that the hips would undergo if the character were walking in a straight line, the number of radians that will be covered during the walking cycle can be calculated. This value is linearly interpolated over the time step of the walking phase to calculate the position and orientation of the hips using Equation 1.16. The other path that comes directly from these calculations is that of the leading heel. A similar process is used to determine the corresponding values that the heel will take during the walking cycle where the centre of orbit is used from the calculation of the hips, as illustrated in Figure 1.7. The radius of the arcs used to drive the heels of the character differs from that of the hips only by a factor of the difference between the model centre of the hips and the femur. The combination of these arc paths result in the ability to smoothly turn the character in either direction at varying rates dependent on changeable parameters such as radius and stride length.

The algorithm to make the character turn is effectively the same as that of walking forward but instead of assuming that the character's hips and leading leg will be moved in a straight line, the path is an arc determined using the technique outlined. This allows the direct application of the heel and toe plants that are used in the forward walking algorithm.
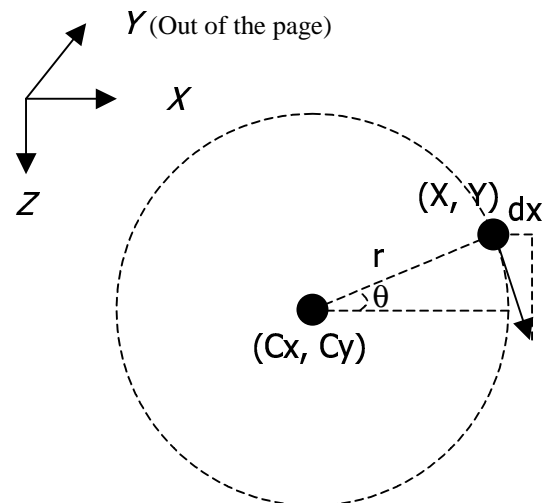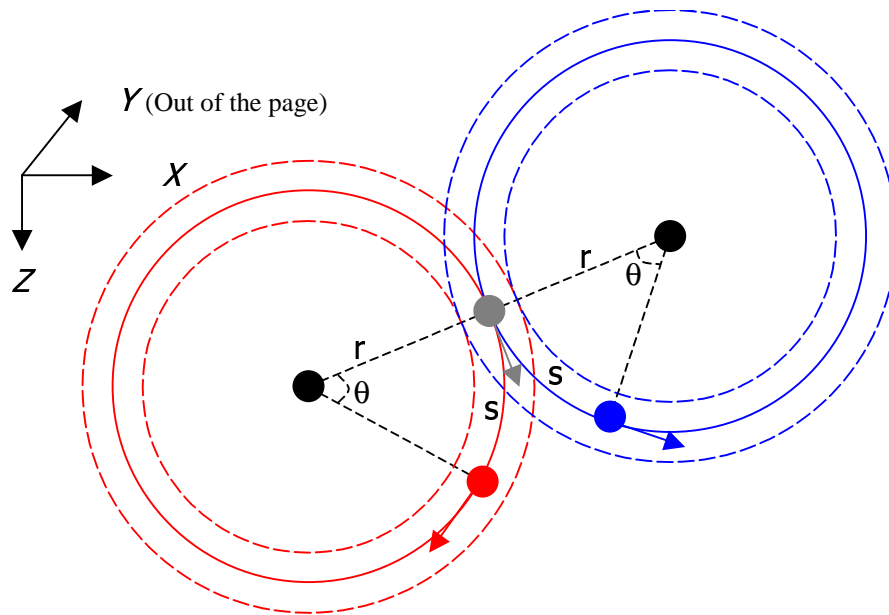

$$\theta = -\sin^{-1}(dx)$$
(turning clockwise about Y-Axis)

$$Cx = X + r\cos\theta$$
$$Cy = Y - r\sin\theta$$

Figure 1.6: Calculating the centre of rotation for turning a character.

Figure 1.7: Calculation of the amount to rotate the character about based on the radius of the circle and stride length. The inner dotted circles represent the path the inside leg would take if it is the leading leg while the dotted outer path is that of the outside leg when leading. The red circles (left) are those when the character turns right while the blue circles (right) represents the character turning left.

- *Other Motion Details*

The character further has the ability to walk smoothly over uneven terrains. This is achieved by determining the ideal position of the hips at the end of a given walk cycle based on the height of the floor at that point and the character's leg length. This distance is linearly interpolated with the current height of the hips during the cycle along with a small sinusoidal wave that gives the effect of the hips naturally moving up and down as the character moves. This difference is also added into the heel height equation for position so that the graph illustrating the heel height in Figure 1.4 is effectively skewed to take into account any varying levels in the ground. The hips are also rotated about the vertical to give the effect of the hips swinging. Both the added hip cycles can be adjusted to give different behaviours – i.e. smaller or larger hip swings.

Weights on the IK chain are also implemented in the IK solver to provide a way of controlling how much each limb within the IK chain is altered comparatively. For example, to prevent the heel of the trailing foot leaving the ground too quickly after it's anchor is removed, more weighting is applied to changing the femur and tibia limbs.

Empirical Results

The results in Table 1.4 are obtained from running *MovingIK* on a Pentium 4 1.4GHz processor with a GeForce2 Ultra. There was a maximum iteration count imposed on the IK solver for the outer loop of 200 cycles while the inner loop was subject to a 20-cycle ceiling. These limits were determined by the empirical running of the IK solver to determine over what limits a solution was very rarely found. The character driven by the user is made up of 18 hierarchical segments where only naturally-occurring DOFs within the human body were permitted. The constraints on each remaining DOF were further limited to joint angles within the scope of normal human movement.

The results given were obtained by driving the character around both flat and uneven terrains. In the case of the uneven terrain, several randomly-generated surfaces were used (including a flight of steps) and the overall results were obtained by averaging the results. Each of the uneven terrains had the same number of vertices and polygons in the model (64,082 polygons compared to 2 polygons for even terrain). The character displayed was that of either a stick figure or a 3D model consisting of 11,101 polygons.

MovingIK was not optimised to use either the half or full Jacobian but instead provided the ability to switch between the two techniques at run-time. There are three different configurations possible to switch between. The first two modes use only the half or full Jacobian respectively to calculate the configuration of the character to position the leading foot and trailing toes. The third mode uses a hybrid approach that uses the full Jacobian to determine the configuration of the leading foot and the half Jacobian to anchor the trailing toes.

The empirical results of driving the computer character within *MovingIK* are illustrated in Table 1.4. It should

be noted that during a single frame, *MovingIK* solves two IK chains – one for each leg. An illustration of *MovingIK* is given in Figure 1.8.

The speed-up factor between the full Jacobian and the half Jacobian, based on the empirical average time per iteration, is 238.5% which when compared to the analytical computed result of 238.9% reinforces the advantages of using the half Jacobian over the full Jacobian whenever possible.

A further conclusion that can be obtained from these results is that the use of the full Jacobian does not necessarily make the IK solver any more stable. This logical conclusion comes form the fact that the analytical speed-up factor calculated assumes that the inner loop is executed an equal number of times for both algorithms. If this were not the case then the empirical results would show a larger difference in speed up factor due to one algorithm executing the inner loop more times than the other.

Conclusions & Future Work

From this analysis of the empirical and analytical results, there is no proven stability advantage over using the full Jacobian. Therefore there is a definite argument for using the half-sized Jacobian when only the position of an end-effector is needed.

As we have shown, there is also scope for using the quicker half Jacobian for limited domains when orientation is required as well as position. Although we have only demonstrated this for a walking motion, this represents one of the most fundamental movements in computer character animation. In other work we have also applied this technique to the field of motion capture retargeting with similarly successful results in both speed and visual accuracy. There are many other conceivable domains in which this application can be used by placing extra dynamic constraints on joint angles to prevent the orientation from deviating too much from

a natural-looking configuration. An arm, for example, would prove just as suitable a subject for the technique.

The advantages of using dynamic constraints to transform an orientation and positional IK problem into a position-only task are a speed-up factor of about 238%. There is also no extra cost to adding in constraints to the half-sized Jacobian algorithm because its framework already operates using joint restrictions. Effectively you get the dynamic constraints for free in the Jacobian-based IK solver.

We have already integrated our quick real-time inverse kinematics solver into a motion capture retargeting application where the next step will be to use the solver to simultaneously individualise the character. For this we are looking into the application of weighted IK chains such that different parts of the articulation change with a varying rate to the others. This would give rise to the very simple and quick production of say injuries or even varying character builds in computer figures.

IK Mode / Measurement	All Half Jacobian (3D X Vector)	All Full Jacobian (6D X Vector)	Hybrid Method
Flat Floor with Stick Character	260 fps	95 fps	115 fps
Flat Floor with Skeleton	140 fps	69 fps	83 fps
Uneven Terrain with Stick Character	97 fps	54 fps	64 fps
Uneven Terrain with Skeleton Character	75 fps	42 fps	53 fps
Average time to execute each IK solver	0.24 ms	5.5 ms	- - - -
Average Number of iterations	18.15	180	- - - -
Average time per iteration	0.013 ms	0.031 ms	- - - -

Table 1.4: Empirical Results from *MovingIK*

REFERENCES

Chin96 K.W. Chin, "Closed-form and generalized inverse kinematic solutions for animating the human articulated structure.", Bachelor's Thesis in Computer Science, Curtin University of Technology, 1996

Crai55 J. J. Craig, "Introduction to Robotics: Mechanics and Control", Addison-Wesley, 1955

Eber01 D. H. Eberly, "3D Game Engine Design", Morgan Kaufmann, 2001

Fedo03 M. Fedor, "Application of Inverse Kinematics for Skeleton Manipulation in Real-time", International Conference on Computer Graphics and Interactive Techniques, p.203-212, 2003

Kwan00 C. Kwang-Jin, K. Hyeong-Seok, "On-line Motion Retargetting", The Journal of Visualization and Computer Animation, Vol. 11, p.223-235, 2000

Lee99 J. Lee, S. Y. Shin, "A Hierarchical Approach to Interactive Motion Editing for Human-Like Figures", Siggraph 99, p.39-48, 1999

Paul88 R. P. Paul, B. Shimano, G. E. Mayer, "Kinematic Control Equations for Simple Manipulators", IEEE Transactions on System, Man & Cybernetics, Vol. 11, No. 6, 1988

Ryck77 J. P. Ryckaert, G. Ciccotti, H. J. C. Berendsen, "Numerical Integration of the Cartesian Equations of Motions of a System with Constraints: Molecular Dynamics of n-Alkanes", Journal of Computational Physics, Vol. 23 p.327-341, 1977

Shin01 H. J. Shin, J. Lee, M. Gleicher, S. Y. Shin, "Computer Puppetry: An Importance-Based Approach", ACM Transactions On Graphics, Vol. 20, No. 2, p.67-94, April 2001

Tang99 W. Tang, M. Cavazza, D. Mountain, R. Earnshaw, "A Constrained Inverse Kinematics Technique for Real-time Motion Capture Animation", The Visual Computer, Vol. 15, p.413-425, 1999

Tola96 D. Tolani, N. I. Badler, "Real-time Inverse Kinematics of the Human Arm", Presence, Vol. 5, No. 4, p.393-401, 1996

Tola00 D. Tolani, A. Goswami, N. Badler, "Real-Time Inverse Kinematics Techniques for Anthropomorphic Limbs", Graphics Models Vol. 62, No. 6, p.353-388, 2000

Wang91 L. Wang, C. Chen, "A Combined Optimisation Method for Solving the Inverse Kinematics Problem of Mechanical Manipulators", IEEE Transactions on Robotics & Applications, Vol. 7, No. 4, p.489-499, 1991

Welm93 C. Welman, "Inverse kinematics and geometric constraints for articulated figure manipulation", Master of Science Thesis, School of Computing Science, Simon Fraser University, 1993

Watt92 A. Watt & M. Watt, "Advanced animation and rendering techniques", Addison-Wesley, 1992

Zhao94 J. Zhao, N. I. Badler, "Inverse Kinematics Positioning Using Nonlinear Programming for Highly Articulated Figures", ACM Transactions on Graphics, Vol. 13, No. 4, p.313-336, 1994
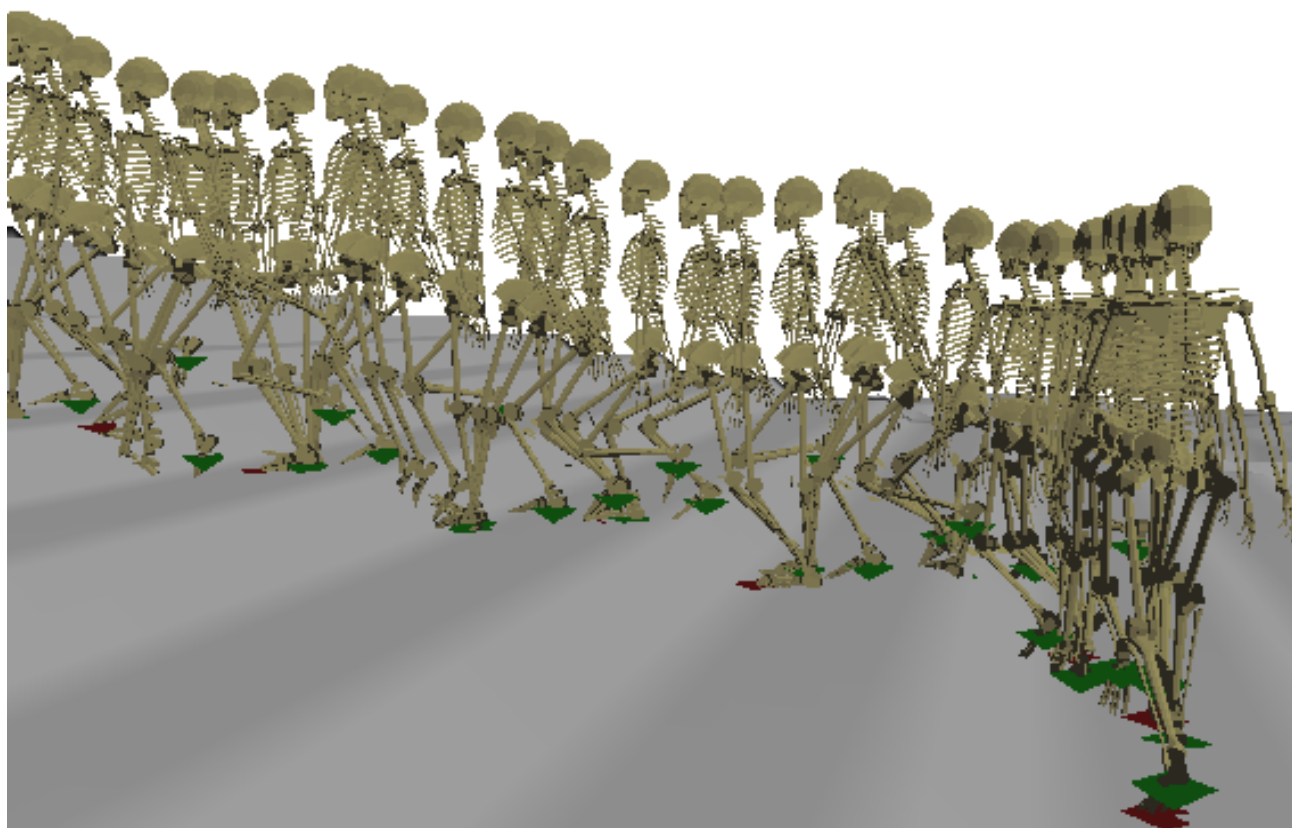
Figure 1.8: Analogue joystick-controlled real-time IK over uneven terrain; green pyramids represent the intended position of the leading foot while the red pyramids indicate desired location of the training toes.

APPENDIX A

C/C++ code snippet for performing the LU decomposition process where um is the upper matrix, *U*, lm is the lower matrix, *L*, and am is the original matrix, *A*.

```
for (i=0; i<6; i++)
{
  um[0][i]=am[0][i];
  lm[i][0]=am[i][0]/um[0][0];
}

for (i=1; i<6; i++)
{
  for (j=i; j<6; j++)
  {
    sum=0;
    for (m=0; m<i; m++)
      sum+=(lm[i][m]*um[m][j]);
    um[i][j]=am[i][j]-sum;
  }

  lm[i][i]=1.0f;
  for (j=i+1; j<6; j++)
  {
    sum=0;
    for (m=0; m<i; m++)
      sum+=(lm[j][m]*um[m][i]);
    lm[j][i]=(am[j][i]-sum)/um[i][i];
  }
}
```

APPENDIX B

C/C++ code snippet for performing the forward and backward substitution required to solve Equation 1.9.

```
for (i=0; i<6; i++)
{
  // Solved the ith column of ym
  for (j=0; j<6; j++)
  {
    sum=0;
    for (m=0; m<j; m++)
      sum+=(lm[j][m]*ym[m]);
    ym[j]=ident[j][i]-sum;
  }
  // Solved the ith column of inverse
  for (j=5; j>=0; j--)
  {
    sum=0;
    for (m=j+1; m<6; m++)
      sum+=(um[j][m]*inverse[m][i]);
    inverse[j][i]=(ym[j]-sum)/um[j][j];
  }
}
```

APPENDIX C

The following C/C++ code calculates an analytical inverse of a general (3 x 3) dimension matrix, *r*.

```
float det=1/
(r[0][0]*(r[1][1]*r[2][2]-r[1][2]*r[2][1])
+r[0][1]*(r[1][2]*r[2][0]-r[1][0]*r[2][2])
+r[0][2]*(r[1][0]*r[2][1]-r[1][1]*r[2][0])
);

inverse[0][0]=
(r[1][1]*r[2][2]-r[2][1]*r[1][2])*det;
inverse[1][0]=
(r[2][0]*r[1][2]-r[1][0]*r[2][2])*det;
inverse[2][0]=
(r[1][0]*r[2][1]-r[2][0]*r[1][1])*det;

inverse[0][1]=
(r[2][1]*r[0][2]-r[0][1]*r[2][2])*det;
inverse[1][1]=
(r[0][0]*r[2][2]-r[2][0]*r[0][2])*det;
inverse[2][1]=
(r[2][0]*r[0][1]-r[0][0]*r[2][1])*det;

inverse[0][2]=
(r[0][1]*r[1][2]-r[1][1]*r[0][2])*det;
inverse[1][2]=
(r[1][0]*r[0][2]-r[0][0]*r[1][2])*det;
inverse[2][2]=
(r[0][0]*r[1][1]-r[1][0]*r[0][1])*det;
```